**Proceedings of the ASME 2020 39th International Conference on Ocean, Offshore and Arctic Engineering**
**OMAE2020**
**August 3-7, 2020, Virtual, Online**

**OMAE2020-18720**



# ACCURACY OF SIMPLIFIED METHODS FOR FATIGUE DAMAGE ESTIMATION OF EXPOSED FISH FARMS

**Martin Slagstad***
Centre for Autonomous Marine Operations and Systems, (NTNU AMOS)
Department of Marine Technology
Norwegian University of Science and Technology, NTNU
NO-7491 Trondheim, Norway
Email: martin.slagstad@ntnu.no

**Pål Takle Bore**
Centre for Autonomous Marine Operations and Systems, (NTNU AMOS)
Department of Marine Technology
Norwegian University of Science and Technology, NTNU
NO-7491 Trondheim, Norway
Email: paal.takle.bore@ntnu.no

**Jørgen Amdahl**
Centre for Autonomous Marine Operations and Systems, (NTNU AMOS)
Department of Marine Technology
Norwegian University of Science and Technology, NTNU
NO-7491 Trondheim, Norway
Email: jorgen.amdahl@ntnu.no

## ABSTRACT

*Fish farms are being placed in more exposed locations than earlier, encouraged by the "development licenses" that the Norwegian Directorate of Fisheries have introduced. Traditional design methods for estimating fatigue damage for fish farms are based on formulations given in the code NS - 9415 Marine fish farms. These methods are initially developed for sheltered areas and may not give an adequate level of safety in more exposed locations, where the dynamic response from waves is of greater importance. Accurate calculations using state of the art methods are very time consuming both with respect to man hours, but especially with regard to CPU consumption. Hence, for practical design, simplified procedures, such as combination of the design wave method with an assumed Weibull distribution, are often used to limit the complexity of the analysis as well as the costs. To the authors knowledge, the accuracy of such simplified methods is not well documented for exposed fish farms and with limited full-scale experience it is difficult to conclude that the desired safety level is achieved. This paper addresses this problem by investigating the accuracy of simplified methods to estimate the fatigue damage. A case study of a modern fish farm concept for exposed waters is performed where the simplified methods are compared to more complex time-domain analyses using state of the art modeling techniques.*

## INTRODUCTION

Accurate methods for estimating the fatigue life of fish farms are important to avoid unexpected failure of the installation. Consequences of such failures can have severe negative environmental effects through fish escape, or in the worst case, human lives may be lost. As fish farms are being located further from shore than earlier it is becoming increasingly important to document the capacities of the structures accurately.

For steel fish farms, NS-9415 [1] requires that a fatigue analysis is performed where loads acting in the wave frequency are taken into account. The current recommendation for conventional fish farms is to assume that the long term stress distribution follows a Weibull distribution unless more accurate analysis is performed. Unless otherwise documented, the shape parameter can be assumed to be 1.0. Further recommendations are not given. The above assumption is identical to the simplified fatigue analyses used for ships in world wide trade and for offshore platforms. Note, that for semi submersible's in the north sea, the Weibull shape parameter is recommended to be 1.1, [2].

Accurate calculations estimating the fatigue life can be performed in the time domain. However, these analyses are time consuming and hence not optimal for design purposes. Simplified analyses as previously described or frequency domain analyses are typically preferred. Without experience or advanced calculations, the simplest method is not suitable for new types of

*Address all correspondence to this author.

structures since the shape factor for the long term stress distribution cannot be known with confidence a priori. Furthermore, analyses in the frequency domain presents additional challenges regarding the representation of the load due to the the assumed linear relationship between the wave height and the response.

The present paper investigates the possibility for using a long term Weibull distribution for fatigue damage estimation for non conventional steel fish farms. The main focus herein is to study the long term stress range distribution in a structural element to determine if the long term history is well modeled with a two parameter Weibull distribution. The structure used as a case study herein is the Ocean Farm 1 (OF1); see Figure 1. The structure is analyzed in USFOS, [3].

**FIGURE 1**. Illustration of the Ocean farming fish farm concept

## LONG TERM STRESS RANGE DISTRIBUTION

In the traditional offshore and ship building industry, simplified methods are often used to calculate the fatigue damage. A widely used method is to assume that the long term stress distribution follows a 2 parameter Weibull distribution, Eqn. (1), with a known shape factor for each particular type of structure.

$$F(x) = 1 - e^{-\left(\frac{x}{q}\right)^h} \tag{1}$$

*q is refferd to as the scale factor, and h, the shape factor.*

The long term distribution of the wave height in the North Sea is often assumed to be well modeled using a 2 parameter Weibull distribution, Eqn. (1) with a shape factor equal to 1, [4]. Battjes, [4], found that the long term distribution of the wave height at 6 of the 7 locations he studied in the Atlantic ocean, North sea and Irish sea followed a Weibull distribution with a shape parameter close to 1.0. The shape factor at Morecambe Bay in the Irish sea was found to be slightly lower than the others, 0.85.

The shape factor is a very important parameter for simplified fatigue estimation since it describes how the stress ranges are distributed. For an identical stress range at a specific return period, a smaller shape factor will give less fatigue damage since the tail of the stress range distribution is more narrow.

Using Morisons equation, Eqn. (2), [5] we can illustrate the relationship between the wave height and the hydrodynamic load. The first term, denoted mass forces, is linearly related to the particle acceleration in the waves and is therefore linearly dependent of the wave height. The second term, drag forces, is dependent on the velocity squared. The drag forces are dependent on the square of the wave height. Assuming that the shape parameter is equal to 1.0 in the long term distribution of the wave height, the shape parameter for the drag forces and inertia forces should be close to 0.5 and 1.0 respectively. The dynamic response of the structure will give some variability.

$$dF = \rho\pi\frac{D^2}{4}C_M a + \frac{1}{2}\rho C_d D u|u| \tag{2}$$

Traditional offshore structures such as ships and floating platforms are mainly affected by the Froude-Krylov and diffraction forces, which are also known as mass forces. The mass forces are linearly dependent of the accelerations. Hence the long term distribution of the loads, and thereby the response, is often well modeled with a Weibull distribution with a shape factor close to 1.0. The shape parameter will have some variability depending on the relationship between the wave height and the load, in addition to the dynamic response of the structure. For slender structures such as jack-ups and jackets, where viscous forces are important, providing a reasonable estimate of the magnitude of the shape parameter is more challenging since the Weibull shape parameter tends to vary between 0.5 and 0.9, [6]. The reduction in shape parameter is due to the relation between the viscous forces and wave height.

A rough estimate of the shape factor for the long term stress distribution for fish farm structures can be determined based on the relationship between the mass and the drag forces. The size of the structure relative to the wave length and wave height is import when considering which forces will dominate, Figure 2, [5]

For the current structure and scatter diagram, Table 1, the maximum ratio, $\frac{H}{D}$, is approximately 3 when the significant wave height is used as H. The fatigue damage is dependent of the entire sea state and it is therefore most relevant to use an average value. If the maximum wave height in the 100 year sea state is considered, the ratio $\frac{H}{D}$ will be equal to approximately 10 for the smallest steel members in the structure when assuming that the maximum wave height is Rayleigh distributed. Hence, for the steel part of the structure the mass term dominates. The diameter of the fish net is very small compared to the wave height, and will have a ratio above 10. It will therefore be drag dominated.

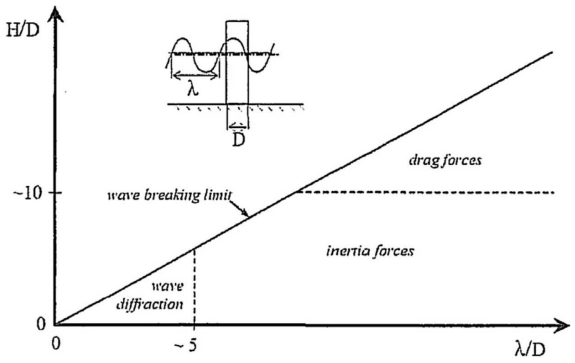


**FIGURE 2**. Dominating wave forces as a function of diameter to wave heigh and diameter to wave length [5]

For fish farm structures, the hydrodynamic load will be a combination of viscous drag forces acting on the fish net and mass forces acting on supporting structures and bouyancy elements. For the OF1 it is expected that the largest contribution is from the mass forces. Based on the above discussion we can estimate that the shape factor for long term stress distribution should be close to 0.8 under the assumption that the long term distribution of the wave height has a shape factor equal to 1.0. The shape factor for the fish farm in [7] was estimated to be between 0.7 and 0.8. This fish farm had more net compared to steel structure and it is therefor reasonable that the shape factor is lower.

Thomassen [7] did not recommend the use of a Weibull distribution for estimating the long term stress distribution and calculating the fatigue damage for tradition fish farm structures. He found that it was difficult to calculate a representative reference stress value such as the 50 year value that produced the correct fatigue damage. It can also be noted that the shape parameters for the long term stress distribution were between 0.7 and 0.8. Bai [8] concluded also that there were other methods more suitable to estimate the long term stress distribution than the 2 parameter Weibull distribution for fatigue estimation. For his case it was found that using the Weibull distribution overestimates the fatigue life.

## NUMERICAL MODELLING, OCEAN FARM 1

Ocean Farm 1 has been designed by combining knowledge from both the Norwegian petroleum and aquaculture industry. Instead of a traditional 'gravity' type cage, using a flexible floating collar and a weight system to support the net, it consists of a rigid frame supporting the net and a superstructure/wheelhouse containing living quarters and rig controls. To avoid drifting off, the structure is kept in place by eight mooring lines. Similar to a semi-submersible platform, it has a high mass relative to the water plane stiffness, giving favorable inertia dominated motion characteristics an illustration of OF1 is given in Figure 1 and Figure 3. A brief description of the structural and hydrodynamic model applied in the numerical analyses follows. As a case study for this paper, the unconventional fish farm structure of the Ocean farm 1 is used.

### Structural model

The members making up the hull structure of OF1 generally consists of slender cylindrical members similar to those found on e.g. jacket structures. All hull members have consequently been modelled as (tubular) three-dimensional beam elements, following recommendations in [9].

The net will also be modelled using three-dimensional beam elements. Special truss elements, which do not carry compression loads, are more commonly used for such members [10], and would probably be a better choice. Numerical issues were however encountered when modelling the net by truss elements, ruling this option out. The use of beam elements will introduce an unrealistically large compression and bending stiffness for the net elements. To compensate, a non-linear material model with lower stiffness for compression than tension have been applied. To keep the computational time within reasonable limits, the net is modelled with a course mesh (in reality, the net consists of millions of individual threads and twines). Each numerical net element is assigned with an *equivalent* cross-sectional area, adding up the areas of the individual threads and ropes it represents. Overall, the structural net model is not considered to cause any errors of significance.

For the mooring lines, truss elements have been applied. Truss elements are considered appropriate due to the negligible bending stiffness of the mooring lines. Such a model is able to simulate both the hanging catenary effect and the line elastic effect — the two mechanisms causing mooring restoring forces [11]. The mooring type is a catenary chain concept with a fibre rope insert at the top. The seabed is modelled by a combination of compression and friction springs.

### Hydrodynamic model

All hull members have a small diameter relative to the expected wave length of the incoming waves. Reflection and diffraction will thus be of minor importance, and Morison's equation can therefore be used to estimate the hydrodynamic loading on the structure [5]. To account for the motion of the structure itself, the following form of Morison's equation, relevant for circular cylinders, is applied (force normal to the axis of the member per unit length) [12]:

$$dF = \rho \frac{\pi D^2}{4}\{C_m a_n - (C_m - 1)\ddot{x}_n\} + \frac{1}{2}\rho D C_d (u_n - \dot{x}_n)|u_n - \dot{x}_n| \quad (3)$$

where $\rho$ is the density of water, $D$ is the outer diameter of the cylinder, $C_m$ and $C_d$ are the inertia and drag coefficients, respectively, $u_n$ and $a_n$ are, respectively, the water particle velocity and acceleration perpendicular to the member, and $\dot{x_n}$ and $\ddot{x_n}$ are the time derivatives of the perpendicular member motion. Based on a compromise between recommended values in [13–15], the inertia and drag coefficients are, respectively, set to 1.5 and 1.05 for all hull members.

The hydrodynamic loading on the mooring lines will also be modelled using the Morison equation Eqn. (3). The drag coefficients are taken as specified in DNVGL-OS-E301 [16], excluding the longitudinal drag. The latter is not considered an issue, particularly since the upper 100 metres of the mooring lines are fibre ropes with negligible longitudinal drag. The inertia coefficient is taken equal 2.0.

For the net structure it is common to use either a Morison model or a screen/panel model. The latter is generally prefered as it is able to deal with the inflow angle dependency of forces on net panels/screens [17]. In addition, experimentally obtained force coefficients for net panels are usually presented as "screen model force coefficients". Such a hydrodynamic model is however not available in the applied analysis software. To circumvent this restriction, the modified Morison model by Bore et al. [18] have been used. This model is based on a simple method for conversion of "screen model force coefficients" to approximate equivalent directional dependent Morison coefficients. Using the (empirically derived) formulas for screen model force coefficients (drag and lift) presented by Løland [19] as the basis, equivalent directional dependent drag and lift coefficients have then been assigned to each net element. The solidity of the net, $Sn = 0.24$. When exposed to a current, the shielding effect from the net panels *upstream* will lead to a reduced incident current velocity on the structural components *downstream*. This is accounted for by assigning all downstream elements with a current velocity reduction factor as given in Løland [19]. Reference is made to [18] for additional details regarding the hydrodynamic model for the net.

## METHODS FOR FATIGUE ESTIMATION

The fatigue damage on a structure can be calculated using several methods. In general, more complicated and time consuming methods give the most accurate estimates, but these are generally not practical for design purposes. In this paper, results from a full time domain analysis are used to estimate the fatigue damage using different approaches.

### Basic assumptions for the analysis

To simplify the analysis, only waves from one heading are considered. The scatter diagram used for the calculations is tabulated in Table 1. The scatter is representative for a specific fish farm site on Norway's coast. The site is exposed to harsher than traditional fish farms have been exposed to in the past. More details regarding the general area of the site location can be found in [20]. The short term variation of the sea states is modelled using a JONSWAP- spectrum with a gamma parameter equal to 3.3. As a simplification the following relation between $T_p$ and $T_z$ is assumed, Tp = 1.25*Tz. For cells spanning more over multiple periods, the mean value of the period is used.

The fatigue damage is calculated using only the axial force in a single member located at the bottom of the structure. The member used in the analysis is shown in red in Figure 3. The force is extracted at a node close to the vertical column in the center of the platform. The force is converted to stress and normalized such that the damage in the most accurate analysis is equal to 1.0. Realistic stress concentrations are not considered herein.

**TABLE 1**. Scatter diagram used for the fatigue analyses

<table>
<tr><th>Tz/Hs</th><th>0.5</th><th>1</th><th>1.5</th><th>2</th><th>2.5</th><th>3</th></tr>
<tr><td>1</td><td rowspan="2"></td><td rowspan="3"></td><td rowspan="3"></td><td rowspan="4"></td><td rowspan="12"></td><td rowspan="4"></td></tr>
<tr><td>2</td><td>3897</td></tr>
<tr><td>3</td><td>2439</td><td>7246</td><td rowspan="2">2587</td></tr>
<tr><td>4</td><td rowspan="2">2027</td><td rowspan="2">1060</td><td rowspan="5">124</td><td rowspan="6">491</td><td rowspan="6">92</td></tr>
<tr><td>5</td></tr>
<tr><td>6</td><td rowspan="2">1778</td><td rowspan="2">240</td></tr>
<tr><td>7</td></tr>
<tr><td>8</td><td rowspan="3">1120</td><td rowspan="3">120</td><td rowspan="5"></td><td rowspan="5"></td><td rowspan="5"></td></tr>
<tr><td>9</td></tr>
<tr><td>10</td></tr>
<tr><td>11</td><td rowspan="2">149</td><td rowspan="2"></td></tr>
<tr><td>12</td></tr>
</table>

For fatigue calculations a single slope SN-curve, Eqn. (4) from [21], is used to estimated the damage. A single slope curve is chosen over the more accurate bi-slope SN-curves to better show the differences in two methods. The absolute value of the damage will not be correct for the structure, but the damages from the analyses are comparable.

$$logN = log\bar{a} - mlog\Delta\sigma \tag{4}$$

N - the number of cycles to failure for a stress range

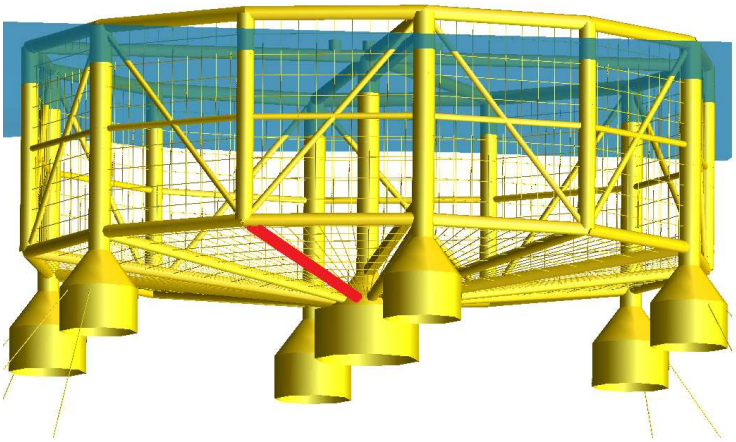

**FIGURE 3**. OF1 seen from below the water line. The axial force is extracted from the red member

$\Delta\sigma$ - Stress range
m - negative inverse slope of SN-curve
$log\bar{a}$ - intercept of logN-axis by SN-curve

## Time domain analysis

The stress history is produced by running a number of time domain analyses. Each of the sea-states in the scatter diagram are analyzed in the time domain until the time derivative of the damage is constant, $\dot{D} = constant$. As Figure 4 shows running the analysis for 1 hour provides an adequate damage estimate. The damage is calculated using three methods presented in the following.

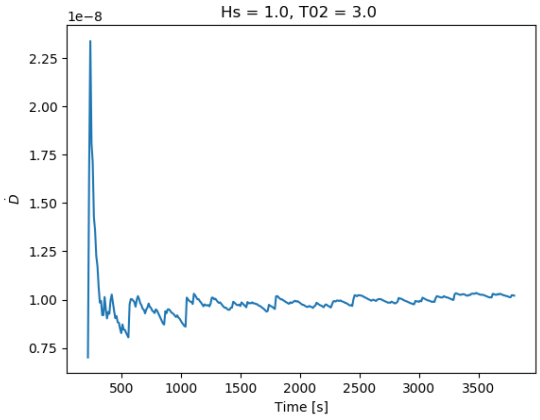


**FIGURE 4**. Time derivative of damage as a function of time for Hs = 1.0 and Tz = 3.0.

**Rainflow** - The stress cycles from the time series are counted using rainflow counting, [22]. The damage for each sea state is calculated using Palmgren-Miner rule, $D = \frac{1}{a}\sum n_i(\Delta\sigma_i)^m$, [6]. The damage from each sea state is scaled to the probability of occurance defined in the scatter diagram, Table 1. The total damage is calculated by summing the contributions from each of the sea states. This is the most accurate method.

**Weibull discrete** - The stress peaks from the time series are detected and used to developed a short term Weibull distribution for the stress cycles for each sea state. The damage from each of the sea states is calculated using Eqn. (5), [21].

$$D = \frac{N}{\bar{a}} q^m \Gamma\left(1 + \frac{m}{h}\right) \tag{5}$$

Here, N is the number of cycles and $\Gamma$ is the gamma function. The total damage is calculated by summing the contributions from each of the sea states.

Peak detection is an important part of establishing the short term distributions for the stress ranges. For calmer sea states the response is quite simple and narrow banded, so the peak detection is straight forward. For the more severe sea states there are often multiple peaks between mean-upcrossings (broad banded) which causes some challenges. For fatigue estimation purposes it is desirable that the mean period of the stress is somewhat similar to the mean period of the waves. The reason is to be able to estimate the number of stress cycles with without performing an analysis for each sea state. The peak picking algorithm is therefore engineered to pick peaks as if the response was narrow banded. In short the algorithm has a limit in time between two neighboring peaks as well as a limit in ratio between to adjacent peaks. An example of the peak detection is shown in Figure 5. The orange dots show all the peaks between mean-up crossings, while the green dots show the peaks that are used for establishing the short term distribution.

The goal of this analysis is to investigate if a short term distribution is able to adequately represent the stress distribution and hence the fatigue damage in a sea state.

**Weibull Long term** - Numerical short term stress range distributions are created for each of the time series. A long term numerical distribution of the stress ranges is created using the short term distributions together with the scatter diagram, Table, 1. A Weibull distribution is fitted to the numerical distribution using a least square fit and probabilites from 6. The fatigue damage is finally calculated using Eqn. (5). The peak detection and the short term distributions for this method are identical to the Weibull discrete method.

The purpose of this method is two fold. The first is to see where if the damage is estimated with a reasonable accuracy and the second, is to see how well the two parameter Weibull

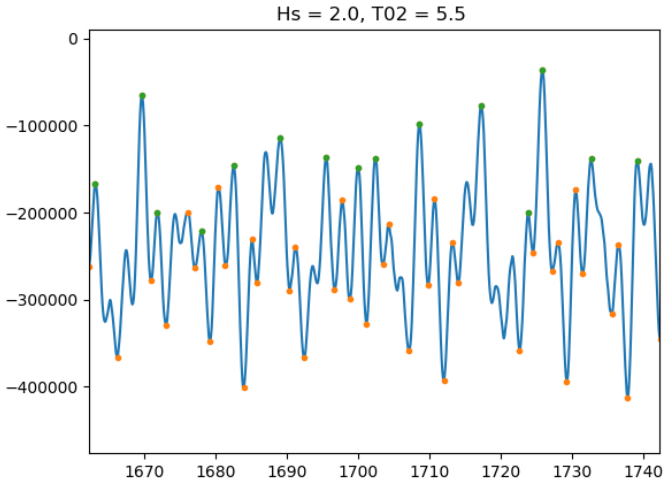


**FIGURE 5**. The orange dots show all the peaks between zero-upcrossings, while the green dots show the peaks used in the short term distribution

distribution fits the long term stress range history.

## WEIBULL DISTRIBUTION OF INDIVIDUAL WAVE HEIGHTS

The long term distribution of the individual wave heights will effect on the long term stress distribution. It is essential that the underlying load distribution is similar if the long term stress distribution is to be similar. The long term distribution of the individual wave heights at the fish farm site is therefore calculated and compared to long term distribution of the individual wave heights in the North Atlantic. The long term distribution of the individual wave heights in the North Atlantic is well modeled with a Weibull distribution with a shape parameter equal to 1.0 [4]. Both cases are calculated herein using a scatter diagram and assuming the the wave heights are Rayleigh distributed in the short term. The scatter diagram for the North Atlantic is found in [13]. It is seen from Figure 7 and 6 that only the tail of the distribution that is Weibull distributed. i.e. the 10 % largest wave heights. This is in line with the methods used to calculate the shape factors in Postresp, [23], and Stofat, [24], which are often used used in the design of floating structures. In both these programs, the long term Weibull distribution is fitted to a number of probabilities of exceedance defined by:

$$P = 10^{-n} \tag{6}$$

where n is an integer between 0 and 12. The shape factor, i.e the slope, is identical for both cases and equal to 1.0. This is in line with the findings of [4]. Another observation is that the fit to the wave heights in the North Atlantic are better than the fitting at the fish farm site.

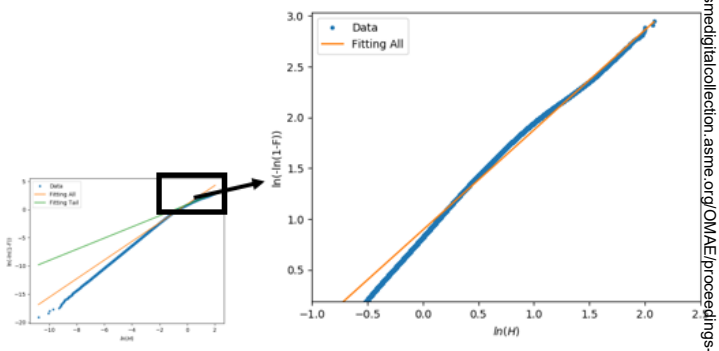


**FIGURE 6**. Accuracy of Weibull fitting for wave heights at the fish farm site

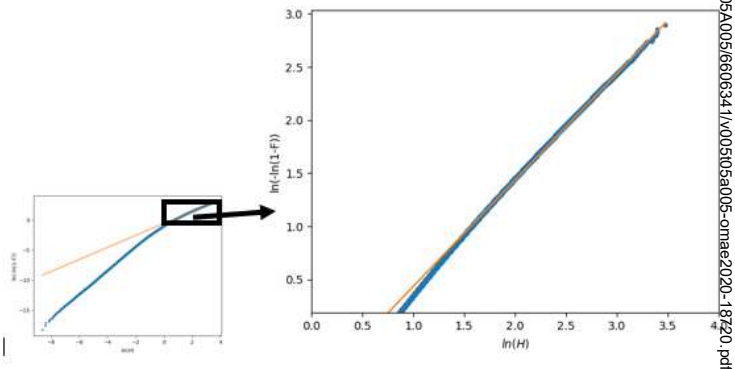


**FIGURE 7**. Accuracy of Weibull fitting for wave heights in the North Atlantic

## PROBABILITY DISTRIBUTION OF THE FATIGUE DAMAGE

In the previous sections it is seen that the assumed long term Weibull distribution of the individual wave height and hence stresses are only accurately represented in the tail of the distribution. For fatigue calculations this raises some concern since the fatigue damage is the sum of the contribution from all the waves. To further investigate this, the probability distribution of the fatigue damage, $f_D(s)$, is created for a single slope SN-curve using

Eqn. (7). The probability distribution is created with two different slopes, m = 3 and m = 5 ref. Eqn. (4). In the following example, a uniform transfer function of unity amplitude is assumed to convert the wave spectrum to a stress range spectrum. The probability density functions for the damage is plotted together with the probability density function for the stress in Figure 8. The long term distribution of the wave heights in the North Atlantic are used in this example.

$$D = \frac{\nu T}{\bar{a}} \int \underbrace{f_s(s)\, s^m}_{f_D(s)} ds \tag{7}$$

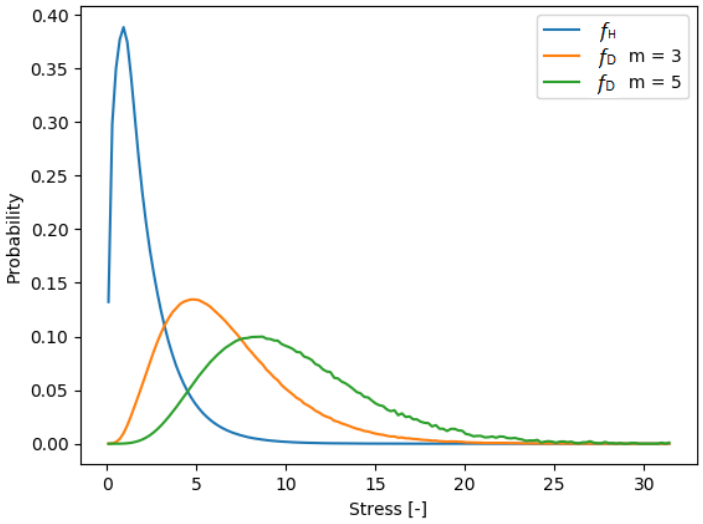


**FIGURE 8**. Damage density functions, $f_D$, based on long term wave height distribution in the North Atlantic plotted together with the probability density function for stress, $f_H$

From Figure 8 it is seen that the damage density functions are shifted right compared to the density function of the stresses. Through this observation, it is seen that the stresses that are important for FLS are significantly greater than the most probable stress. The stated observation is essential for an accurate estimate of the fatigue damage since the fitting of the long term stress distribution is only performed for the tail of the long term distribution. i.e, the fitted long term distribution is not accurate for all stress ranges.

From Figure 7 it is seen that Weibull distribution has a good fit to the 20% largest responses. The stress value with an exceedance probability equal to 20 % is referred to as $S_{20}$. Using the distribution functions presented in Figure 8 it is found that 88 % of the area of the damage distribution, $f_D$, with m = 3 is above $S_{20}$. For the damage distribution, $f_D$, with m = 5 the fraction is 98 %. Based on this observation it is expected that the simplified Weibull approach can accurately estimate the fatigue damage even if only the upper part of the long term distribution is well modeled with the assumed Weibull distribution.

## RESULTS

### Full Analysis rain flow discrete

The results from the full analysis using rain flow counting is shown in Table 2. The results produced using this method are considered to be the most accurate. The total damage is therefore normalized to 1.0. The Table shows that the majority of the damage comes from sea states with a high probability of occurrence in addition to the two largest sea states.

**TABLE 2**. Results from full Fatigue analysis with rain flow counting

| Hs | Tm02 | Fraction | Damage | Factored damage |
|---|---|---|---|---|
| 0.5 | 2 | 0.17 | 7.22E-6 | 0.21 |
| 0.5 | 3 | 0.104 | 2.07E-7 | 3.8E-3 |
| 0.5 | 4.5 | 8.70E-2 | 2.75E-8 | 4.20E-4 |
| 0.5 | 6.5 | 7.60E-2 | 1.08E-7 | 1.4E-3 |
| 0.5 | 9 | 4.80E-2 | 1.49E-6 | 0.01 |
| 0.5 | 11.5 | 6.00E-3 | 8.12E-7 | 8.5E-4 |
| 1 | 3 | 0.31 | 6.03E-6 | 0.33 |
| 1 | 4.5 | 4.50E-2 | 6.93E-7 | 0.01 |
| 1 | 6.5 | 0.01 | 3.04E-6 | 0.01 |
| 1 | 9 | 5.00E-3 | 4.74E-5 | 0.04 |
| 1.5 | 3.5 | 0.11 | 8.07E-6 | 0.16 |
| 1.5 | 6 | 5.00E-3 | 1.34E-5 | 0.01 |
| 2 | 5.5 | 2.10E-2 | 2.37E-5 | 0.09 |
| 3 | 5.5 | 4.00E-3 | 1.88E-4 | 0.13 |

### Full Analysis Weibull discrete

The method used here is similar to the full fatigue analysis with rain flow counting. The only difference is how the damage in the different sea states is calculated. Hence the ratio of the damage Weibull/rainflow for each of the sea states is presented

in Table 3. It is seen that most of the sea states with a period less the 6 seconds are within 10% of the damage calculated with the rain flow method. This gives a strong indication that the two parameter Weibull distribution is adequate for the short term distribution of the stress range. One of the fittings for the short term stress distributions is shown in Figure 10.

For the sea-states with periods greater than 6 seconds it is seen that the short term Weibull distribution underestimates the damage compared to the rain flow-method. It is believed that the main reason is due to convergence issues. With a longer average period, the number of cycles will be less, and hence the analysis should have been run longer. It is however seen that these sea states have only a small contribution to the total damage due to their low probability of occurrence. The results are therefor accepted as they are. The convergence error affects both the Weibull and the rain flow estimates.

It is also seen that the Weibull distribution does not fit the sea-states with long periods as well as for the shorter periods. Figure 9 shows the worst Weibull fitting. The Figure shows that the most severe sea states are under-estimated by the fitted distribution. It is therefore expected that the damage should be somewhat under predicted.

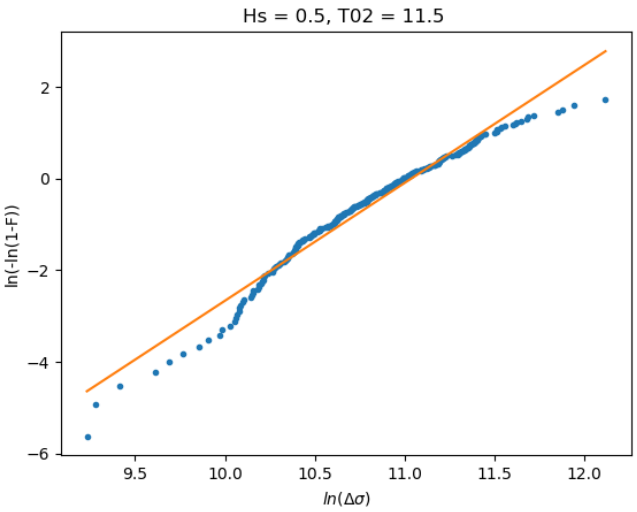


**FIGURE 9**. Short term Weibull fitting for Hs = 0.5 and Tm02 = 11.5

The total damage using this method is 0.99, which is in practice identical to the rainflow method.

The fitted Weibull parameters together with an estimate of the zero up crossing period is presented in Table 4. It is seen that the shape parameter is slightly above 2 for all of the sea states, i.e. approximately Rayleigh distributed. Another observation is that $\bar{T}_{m02}$ is fairly similar to $T_{m02}$. The average stress period

**TABLE 3**. Damage ratio ($D_w/D_{rf}$) for each sea state. $D_w$ and $D_{rf}$ are the damage estimates using a Weibull distribution and rain flow counting respectively.

| Hs | $T_{m02}$ | $D_w/D_{rf}$ |
|---|---|---|
| 0.5 | 2 | 1.17 |
| 0.5 | 3 | 1.06 |
| 0.5 | 4.5 | 1.00 |
| 0.5 | 6.5 | 0.83 |
| 0.5 | 9 | 0.65 |
| 0.5 | 11.5 | 0.61 |
| 1 | 3 | 0.95 |
| 1 | 4.5 | 0.98 |
| 1 | 6.5 | 0.80 |
| 1 | 9 | 0.64 |
| 1.5 | 3.5 | 1.04 |
| 1.5 | 6 | 0.85 |
| 2 | 5.5 | 0.92 |
| 3 | 5.5 | 0.94 |

for the stress range in the long term is only 7% lower than the average period of the wave heights. The average period for the stress range is 3.01 s compared to 3.24 s for the wave heights.

$$\bar{T}_{m02} = \frac{t_{simulation}}{N_{peaks}} \tag{8}$$

## Long term Weibull distribution based on numerical short term distributions

The fitted long term distribution of the stress range is shown in Figure 11. The Weibull distributions is fitted to the upper tail using the probabilities from Eqn. (6). The $n$ values used to fit the distribution are; 2, 3, 4 and 5. The damaged estimated from the long term distribution is 0.64. Hence, the damage is underestimated by 36 % which is significant. In the calculations, the correct number of stress cycles is taken directly from the short term distributions and is therefor not an error source. The shape parameter in the Weibull distribution is equal to 0.85, and is in line with expectations. It is seen that the Weibull distribution fits the tail with a reasonable accuracy. However, the length of

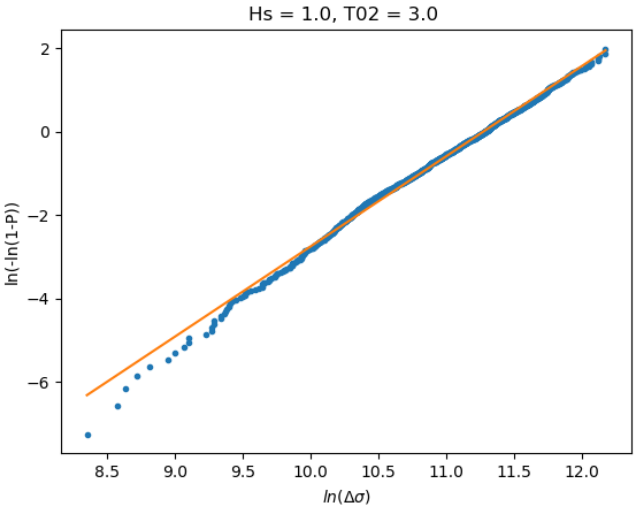


**FIGURE 10**. Short term fitting for Hs = 1 and Tz = 3

**TABLE 4**. Weibull parameters for the short term sea states.

| Hs | $T_{m02}$ | Shape | Scale | $\bar{T}_{m02}$ |
|---|---|---|---|---|
| 0.5 | 2 | 2.00 | 69897 | 2.40 |
| 0.5 | 3 | 2.21 | 36071 | 2.65 |
| 0.5 | 4.5 | 2.35 | 25055 | 3.01 |
| 0.5 | 6.5 | 2.3 | 38967 | 8.8 |
| 0.5 | 9 | 2.29 | 65244 | 10.62 |
| 0.5 | 11.5 | 2.57 | 62002 | 13.00 |
| 1 | 3 | 2.25 | 69296 | 2.56 |
| 1 | 4.5 | 2.42 | 48123 | 2.96 |
| 1 | 6.5 | 2.33 | 75955 | 8.80 |
| 1 | 9 | 2.34 | 130956 | 10.71 |
| 1.5 | 3.5 | 2.228 | 77338 | 2.91 |
| 1.5 | 6 | 2.41 | 100562 | 7.09 |
| 2 | 5.5 | 2.43 | 113980 | 6.84 |
| 3 | 5.5 | 2.37 | 171595 | 6.84 |

the tail with a constant slope is quite short when comparing to Figure 7. It is also seen that the transition is more distinct. The difference in tail behavior is believed to be the reason for the inaccurate fatigue estimate.

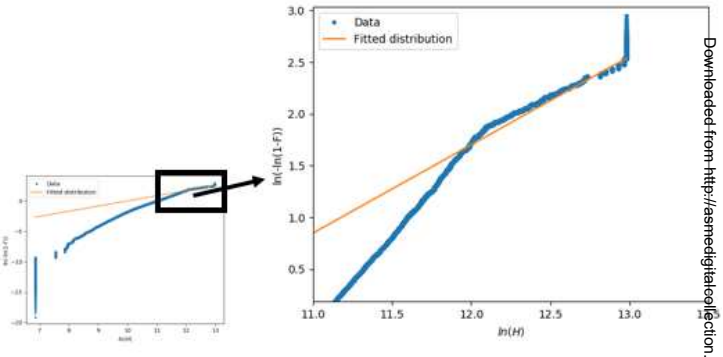


**FIGURE 11**. Accuracy of the Weibull fitting for the long term stress range distribution

## DISCUSSION

It is seen that the short term Weibull distributions are able to estimate the damage from each sea state with reasonable accuracy for almost all sea states. Hence, the practical engineering approach used for the peak detection seems to provide a good estimation of the fatigue damage. There were however some problems with damage convergence for the sea states with a large mean period. It would be beneficial to run these analyses longer to make a solid conclusion regarding the short term distributions of the stress cycles.

For the long term distribution it is seen that the shape factor is in line with expectations. The damage is however greatly underestimated. The reason is believed to be that the tail of the distribution is too short and distinct. It is a possibility that the scatter diagram is too coarse in the region that produces the largest stress cycles. This is supported by the differences in the tail in Figure 7 and 6. A finer scatter diagram may alter the shape of the tail. It may however be that the physics are not in line with the method used.

## CONCLUSION

The use of a long term Weibull distribution for estimating the fatigue damage of a non-conventional fish farm structure cannot be recommended based on the findings herein. The method is not able to predict the damage with reasonable accuracy. There is however some hope that this method may be used. There are two main reason for this. The first is that the average period of the stress range is similar to the average period of the waves. For design purposes a contingency of 10-15 % could be added to the number of wave cycles for a reasonably good estimate of the stress cycles. The second reason is that the slope of the Weibull distribution is in line with the a priori expectations.

## ACKNOWLEDGEMENT

This work was supported by the Research Council of Norway through the Centre of Excellence funding scheme, NTNU AMOS, project number 223254.

## REFERENCES

[1] Standards Norway, 2009. "Norwegian Standard NS 9415.E:2009 Marine fish farms - Requirements for site survey, risk analyses, design, dimensioning, production, installation and operation".

[2] DNVGL, 2015. "DNVGL-RP-C103 Column-Stabilised Units".

[3] Søreide, T. H., Amdahl, J., Eberg, E., Holmås, T., and Øyvind Hellan, 1988. *USFOS – A Computer Program for Progressive Collapse Analysis of Steel Offshore Structures. Theory Manual.* SINTEF, www.usfos.no, Oct.

[4] Battjes, J. A., 1972. "Long-term wave height distributions at seven stations around the British Isles". *Deutsche Hydrographische Zeitschrift,* ***25***(4), pp. 179–189.

[5] Odd M. Faltinsen. *Sea Loads on Ships and Offshore Structures*. Cambridge university press.

[6] Inge Lotsberg. *Fatigue Design of Marine Struvtures*. Cambridge university press.

[7] Thomassen, P. E., 2008. *Methods for Dynamic Response Analysis and Fatigue Life Estimation of Floating Fish Cages*.

[8] Bai, X.-d., 2018. "Investigation on the Probabilistic Distribution of the Stress Range of Net Cage Floater of Fish Cage for Fatigue Life Prediction". pp. 1–8.

[9] NORSOK, 2013. *NORSOK N-004, Design of Steel Structures*. Standards Norway.

[10] Moe, H., Fredheim, A., and Hopperstad, O., 2010. "Structural analysis of aquaculture net cages in current". *Journal of Fluids and Structures,* ***26***, pp. 503–516.

[11] DNV, 2010. *DNV-RP-F205, Global Performance Analysis of Deepwater Floating Structures*. Det Norske Veritas.

[12] Næss, A., and Moan, T., 2012. *Stochatic Dynamics of Marine Structures*. Cambridge University Press.

[13] DNV, 2014. *DNV-RP-C205, Environmental conditions and environmental loads*. Det Norske Veritas.

[14] Clauss, G., Lehmann, E., and Østergaard, C., 1992. *Offshore Structures Volume I - Conseptual Design and Hydromechanics*. Springer-Verlag.

[15] Sarpkaya, T., 1976. "Forces on rough-walled circular cylinders in harmonic flow". *Coastal Engineering*, pp. 2301–2320.

[16] DNVGL, 2015. *DNVGL-OS-E301 Position mooring*. DNV GL.

[17] Kristiansen, T., and Faltinsen, O. M., 2012. "Modelling of current loads on aquaculture net cages". *Journal of Fluids and Structures,* ***34***, pp. 218–235.

[18] Bore, P. T., Amdahl, J., and Kristiansen, D., 2017. "Modelling of hydrodynamic loads on aquaculture net cages by a modified Morison model". *7th International Conference on Computational Methods in Marine Engineering, MARINE 2017*, pp. 647–662.

[19] Løland, G., 1991. "Current forces on and flow through fish farms". PhD thesis, Division of Marine Hydrodynamics, The Norwegian Institute of Technology.

[20] Bore, P. T., and Amdahl, J., 2017. "Determination of environmental conditions relevant for the Ultimate limit state at an exposed aquaculture location". pp. 1–14.

[21] DNVGL, 2014. "RP-C203 Fatigue design of offshore steel structures".

[22] Downing, S. D., and Socie, D. F., 1982. "Simple rainflow counting algorithms". *International Journal of Fatigue,* ***4***(1), pp. 31–40.

[23] DNV, and Veritas, D. N., 2004. "SESAM User Manual Postresp: Interactive Postprocessor for General Response Analysis".

[24] DNV, and Veritas, D. N., 2009. "SESAM User Manual STOFAT: Fatigue Damage Calculation of Welded Plates and Shells, version 3.4".